International Journal of Mechanical Sciences 133 (2017) 504–512

Contents lists available at ScienceDirect

International Journal of Mechanical Sciences

journal homepage: www.elsevier.com/locate/ijmecsci

Dynamic response and vibration of composite double curved shallow shells with negative Poisson's ratio in auxetic honeycombs core layer on elastic foundations subjected to blast and damping loads

Nguyen Dinh Duc[a,b,c,*], Kim Seung-Eock[c], Pham Hong Cong[a,d], Nguyen Tuan Anh[a], Nguyen Dinh Khoa[a]

[a] Advanced Materials and Structures Laboratory, VNU, Hanoi University of Engineering and Technology (UET), 144-Xuan Thuy Cau Giay, Hanoi, Viet Nam
[b] Infrastructure Engineering Program, VNU, Hanoi, Vietnam-Japan University (VJU), My Dinh 1 Tu Liem, Hanoi, Viet Nam
[c] National Research Laboratory, Department of Civil and Environmental Engineering, Sejong University, 209 Neungdong-ro, Gwangjin-gu, Seoul 05006, South Korea
[d] Centre for Informatics and Computing (CIC), Vietnam Academy of Science and Technology, 18 Hoang Quoc Viet Cau Giay, Hanoi, Viet Nam

ARTICLE INFO

Keyword:
Dynamic response and vibration
Composite double curved shallow shells
Auxetic honeycombs core layer with negative Poison's ratio
FSDT
Blast and damping loads
Elastic foundations

ABSTRACT

The purpose of the present study is to investigate dynamic response and vibration of composite double curved shallow shells with negative Poisson's ratios in auxetic honeycombs core layer on elastic foundations subjected to blast and damping loads using analytical solution. This study considers composite double curved shallow shells with auxetic core which have three layers in which the top and bottom outer skins are isotropic aluminum materials; the central layer has honeycomb structure using the same aluminum material. Based on the first order shear deformation theory (FSDT) with the geometrical nonlinear in von Karman and using Airy stress functions method, Galerkin method and the fourth-order Runge–Kutta method, the resulting equations are solved to obtain expressions for nonlinear motion equations. The effects of geometrical parameters, material properties, elastic foundations Winkler and Pasternak, the nonlinear dynamic analysis and vibration of double curved shallow shells with negative Poisson's ratios in auxetic honeycombs core layer are studied.

1. Introduction

Auxetic materials were discovered over 100 years ago [1,2]. Most natural materials are characterized by a positive Poisson's ratio, namely they are observed to contract (expand) laterally when stretched (compressed) longitudinally. Nonetheless, the classical theory of elasticity does not preclude the existence of materials with negative Poisson's ratio, known as 'auxetic' after Ref. [3].

In recent years, there have been many studies on composite auxetic material with negative Poisson's ratio. Lu et al. [4] investigated the elastic properties of two novel auxetic 3D cellular structures. Kwon and Phan [5] studied the composites with auxetic inclusions showing both an auxetic behavior and enhancement of their mechanical properties. Assidi and Ganghoffer [6] considered the composites with auxetic inclusions showing both an auxetic behavior and enhancement of their mechanical properties, and the hexachiral and hexagonal reentrant lattices are considered as representative of the two main deformation mechanisms responsible for auxeticity. Bhullar et al. [7] investigated the auxetic behavior of a thermoelastic layered plate. Burlayenko and Sadowski [8] analyzed the effective elastic properties of foam-filled honeycomb cores of sandwich panels. Grima et al. [9] studied the hexagonal honeycombs with zero Poisson's ratios and enhances stiffness. Milton [10] considered the composite materials with Poisson's ratios close to −1. Yang et al. [11] investigated the geometric effects on micropolar elastic honeycomb structure with negative Poisson's ratio using the finite element method. Prawoto [12] presented a review on structures with the negative Poisson's ratio. Liu et al. [13] presented the wave propagation in a sandwich plate with a periodic composite core. Jopek and Strek [14] investigated the thermal and structural dependence of auxetic properties of composite materials. Wan et al. [15] investigated the study of negative Poisson's ratios in auxetic honeycombs based on a large deflection model. Grujicic et al. [16] studied the multi-physics modeling of the fabrication and dynamic performance of all-metal auxetic-hexagonal sandwich-structures. Qing-Tian and Zhi-Chun [17] presented the wave propagation in sandwich panel with auxetic core. Cielecka and Jędrysiak [18] studied the non-asymptotic model of dynamics of honeycomb lattice-type plates. Lewiński [19] investigated the physical correctness of Cosserat type

* Corresponding author at: Advanced Materials and Structures Laboratory, VNU, Hanoi University of Engineering and Technology (UET), 144-Xuan Thuy Cau Giay, Hanoi, Viet Nam.
E-mail address: ducnd@vnu.edu.vn (N.D. Duc).

http://dx.doi.org/10.1016/j.ijmecsci.2017.09.009
Received 15 March 2017; Received in revised form 17 August 2017; Accepted 9 September 2017
Available online 13 September 2017
0020-7403/

models of honeycomb grid plates. Wierzbicki and Woźniak [20] considered the dynamic behavior of honeycomb based composite solids.

In recent years, the safety of buildings and structures of infrastructure has become hot issues all over the world because the negative dynamic loads caused increase in terrorist activities, accidental blast. Imbalzano et al. [21] studied the auxetic composite panels under blast loading. Imbalzano et al. [22] studied the blast resistance of auxetic and honeycomb sandwich panels: Comparisons and parametric designs. Li et al. [23] studied the finite element analysis of sandwich panels with stepwise graded aluminum honeycomb cores under blast loading. Lam et al. [24] investigated the response spectrum solutions for blast loading. Qi et al. [25] studied dynamic response and optimal design of curved metallic sandwich panels under blast loading. Schenk et al. [26] analyzed the novel stacked folded cores for blast-resistant sandwich beams. Duc et al. [27] studied the nonlinear dynamic response and vibration of imperfect shear deformable functionally graded plates subjected to blast and thermal loads. Tan et al. [28] presented the blast-wave impact mitigation using negative effective mass density concept of elastic metal materials. In recent years, there have had some studies [29] which investigated the nonlinear dynamic response and vibration of sandwich composite plates with negative Poisson's ratio in auxetic honeycombs (but have not actually studied the double curved shallow shells yet). Ghaznavi and Shariyat [30] analyzed the non-linear layerwise dynamic response analysis of sandwich plates with soft auxetic cores and embedded SMA wires experiencing cyclic loadings (using numerical method).

Research on the nonlinear vibration and dynamic response of double curved shallow shells has done quite a few (but the shell made of auxetic material has not been studied yet). Quan and Duc [31] studied the vibration and dynamic response of shear deformable imperfect functionally graded double curved shallow shells resting on elastic foundations in thermal environments. Duc and Quan [32] presented the nonlinear dynamic analysis of imperfect FGM double curved thin shallow shells with temperature-dependent properties on elastic foundation. Chorfi and Houmat [33] investigated the nonlinear free vibration of a functionally graded doubly curved shallow shell of elliptical planform. Bich et al. [34] studied the nonlinear vibration of imperfect eccentrically stiffened functionally graded double curved shallow shells resting on elastic foundation using the first order shear deformation theory. In 2014, Duc [37] published a valuable book "Nonlinear static and dynamic stability of functionally graded plates and shells", in which the results of nonlinear dynamic analysis of shear deformable FGM structures on elastic foundations.

The researches only focus on the structure of the core layer in auxetic materials (structure, material parameters, optimum …), the others investigate nonlinear dynamic response of double curved shallow FGM shells [31–37]. The first nonlinear dynamic response of auxetic structure under blast using analytical method was conducted on plate [29], the auxetic shell has not been published yet. From above, it can be seen that there has not got any research using analytical method to study the nonlinear dynamic response of the double curved shallow shells with negative Poisson's ratios in auxetic honeycombs on elastic foundations subjected to blast. The advantage of analytical method is that the results are shown explicitly in the input parameters, therefore we can actively control the behavior of the shells by selecting those parameters appropriately.

The paper focuses on studying the vibration and dynamic response of the composite double curved shallow shells with negative Poisson's ratio in auxetic honeycombs layer on elastic foundations subjected to blast and damping loads using analytical solution. The double curved shallow shells used in the paper have three layers in which the top and bottom outer skins are isotropic aluminum materials; the central layer has honeycomb structure using the same aluminum material. The governing equations are derived within the framework of the Reddy's first order shear theory, accounting for both the von - Karman nonlinearity. The work also analyzes and discusses the effects of material and geometrical properties, elastic foundations, mechanical, blast and damping loads on the nonlinear dynamic response of the double curved shallow shells with negative Poisson's ratio in auxetic honeycombs.

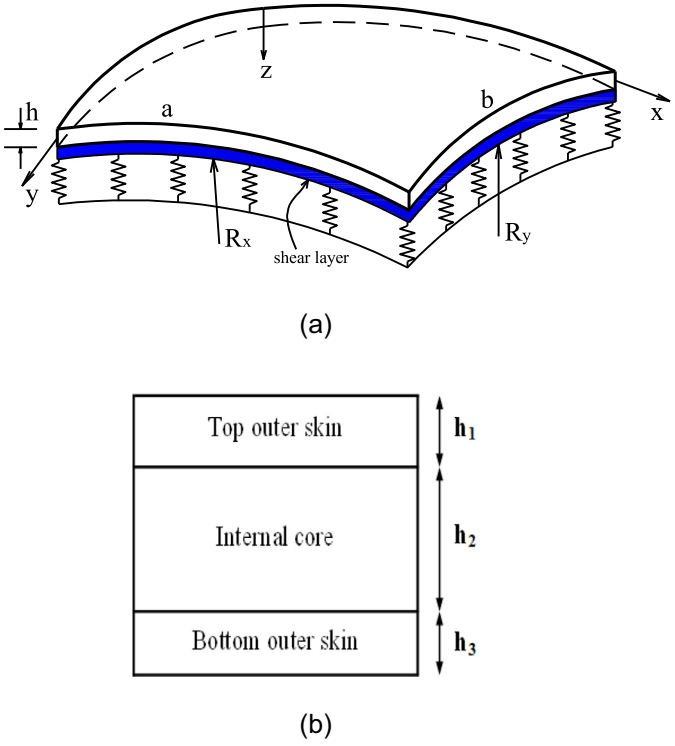

Fig. 1. (a) Model of sandwich composite double curved shallow shell with auxetic core layer on elastic foundations. (b) Discretization of double curved shallow shell.

2. Composite double curved shallow shell with auxetic core model

2.1. Model

Considering a composite double curved shallow shell with auxetic core layer of radius of radii of curvature R_x, R_y, length of edges a, b and uniform thickness h resting on elastic foundations, a coordinate system (x, y, z) is established, in which the (x, y) plane is in the middle surface of the shell and z is in the thickness direction (Fig. 1a). The auxetic core has three layers in which the top and bottom outer skins are isotropic aluminum materials; the central layer has honeycomb structure using the same aluminum material (Fig. 1b). The bottom outer skin thickness is h_1, internal honeycomb core material thickness is h_2 and the top outer skin thickness is h_3, and the total thickness of the shell is $h = h_1 + h_2 + h_3$.

The reaction–deflection relation of Pasternak foundation is given by

$$T_0 = K_1 w - K_2 \nabla^2 w \tag{1}$$

in which $\nabla^2 = \frac{\partial^2}{\partial x^2} + \frac{\partial^2}{\partial y^2}$, w is the deflection of the double curved shallow shell, K_1 and K_2 are Winkler foundation modulus and shear layer of Pasternak foundation, respectively [36,37].

2.2. Honeycomb core materials

The double curved shallow shells with the auxetic honeycomb core layer with negative Poisson's ratio are introduced in this paper. Unit cells of core material discussed in the paper are shown in Fig. 2 where l is the length of the inclined cell rib, h is the length of the vertical cell rib, θ is the inclined angle, α and β define the relative cell wall length and the wall's slenderness ratio, respectively, which are important parameters in honeycomb property.

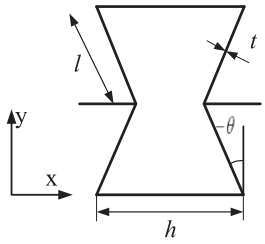

Fig. 2. Geometric of the cell of honeycomb core layer.

Table 1
Poisson's ratio v_{12} in auxetic honeycombs of the double curved shallow shell at the limit value of small deformation.

	$\frac{h}{l}=1$	$\frac{h}{l}=1.5$	$\frac{h}{l}=2$	$\frac{h}{l}=2.5$	$\frac{h}{l}=3$
$\theta=-35$	−2.7434	−1.2628	−0.8201	−0.6073	−0.4821
$\theta=-45$	−2.4142	−0.8918	−0.5469	−0.3944	−0.3084
$\theta=-50$	−2.3054	−0.7349	−0.4371	−0.3111	−0.2414
$\theta=-55$	−2.2208	−0.5899	−0.3401	−0.2389	−0.1842
$\theta=-75$	−2.0353	−0.1299	−0.0671	−0.0452	−0.0341

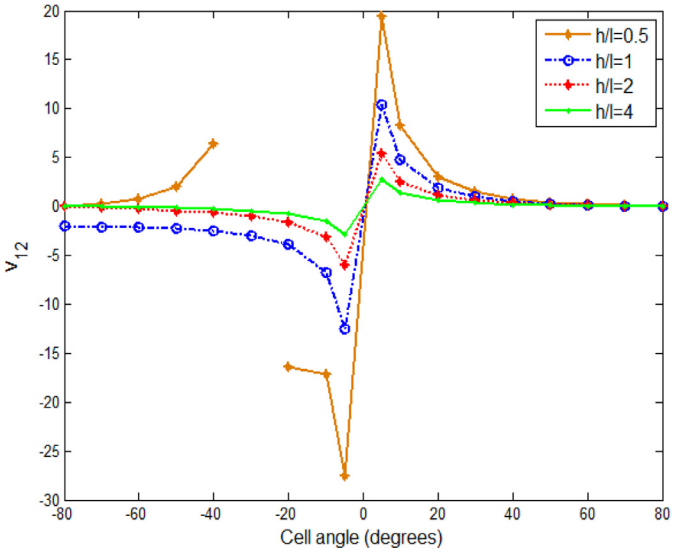

Fig. 3. Poisson's ratio versus cell inclined angle with different cell aspect ratio $\frac{h}{l}$.

Formulas in Ref. [17] are adopted for calculation of honeycomb core material property

$$E_1^C = E\left(\frac{t}{l}\right)^3 \frac{\cos\theta}{\left(\frac{h}{l}+\sin\theta\right)\sin^2\theta},\quad E_2^C = E\left(\frac{t}{l}\right)^3 \frac{\left(\frac{h}{l}+\sin\theta\right)}{\cos^3\theta},$$

$$v_{12}^C = \frac{\cos^2\theta}{\left(\frac{h}{l}+\sin\theta\right)\sin\theta},\quad G_{12}^C = E\left(\frac{t}{l}\right)^3 \frac{\left(\frac{h}{l}+\sin\theta\right)}{\left(\frac{h}{l}\right)^2\left(1+2\frac{h}{l}\right)\cos\theta},$$

$$G_{13}^C = G\frac{t}{l}\frac{\cos\theta}{\left(\frac{h}{l}+\sin\theta\right)},\quad G_{23}^C = G\frac{t}{l}\frac{1+2\sin^2\theta}{2\cos\theta\left(\frac{h}{l}+\sin\theta\right)},$$

$$\rho^C = \rho\frac{t/l(h/l+2)}{2\cos\theta(h/l+\sin\theta)} \tag{2}$$

where symbol "C" represents core material, E, G and ρ are Young's moduli, shear moduli and mass density of the origin material.

The effects of geometry of double curved shallow shells with negative Poisson's ratio v_{12} at the limit of small deformation are presented in Table 1 and Fig. 3 for the combinations of θ and $\frac{h}{l}$. From Table 1 and Fig. 3, it can be seen that Poisson's ratio v_{12} increased when geometric parameters of $\frac{h}{l}$ increase and vice versa. The same for in the case geometric parameters of θ decreases, Poisson's ratio v_{12} increased and vice versa.

3. Theoretical formulations

In the present study, the first order shear deformation theory (FSDT) is used to derive the governing equations and determine the blast load of the composite double curved shallow shell with negative Poisson's ratio in auxetic honeycombs.

The strain–displacement relations taking into account the von Karman nonlinear terms are [35-38]:

$$\begin{Bmatrix}\varepsilon_x\\ \varepsilon_y\\ \gamma_{yz}\\ \gamma_{xz}\\ \gamma_{xy}\end{Bmatrix} = \begin{Bmatrix}\varepsilon_x^0\\ \varepsilon_y^0\\ \gamma_{yz}^0\\ \gamma_{xz}^0\\ \gamma_{xy}^0\end{Bmatrix} + z\begin{Bmatrix}\varepsilon_x^1\\ \varepsilon_y^1\\ \gamma_{yz}^1\\ \gamma_{xz}^1\\ \gamma_{xy}^1\end{Bmatrix}$$

$$= \begin{Bmatrix}\frac{\partial u}{\partial x}+\frac{1}{2}\left(\frac{\partial w}{\partial x}\right)^2-\frac{w}{R_x}\\ \frac{\partial v}{\partial y}+\frac{1}{2}\left(\frac{\partial w}{\partial y}\right)^2-\frac{w}{R_y}\\ \frac{\partial w}{\partial y}+\phi_y\\ \frac{\partial w}{\partial x}+\phi_x\\ \frac{\partial u}{\partial y}+\frac{\partial v}{\partial x}+\frac{\partial w}{\partial x}\frac{\partial w}{\partial y}\end{Bmatrix} + z\begin{Bmatrix}\frac{\partial \phi_x}{\partial x}\\ \frac{\partial \phi_y}{\partial y}\\ 0\\ 0\\ \frac{\partial \phi_x}{\partial y}+\frac{\partial \phi_y}{\partial x}\end{Bmatrix} \tag{3}$$

In the above equations, u, v, w are displacement components corresponding to the coordinates(x, y, z), and φ_x, φ_y are the rotations of normals to the mid-surface with respect to x and y axes, respectively.

Hooke's law for the curved shallow shells with negative Poisson's ratio in auxetic honeycombs is defined as follows [29]

$$\begin{Bmatrix}\sigma_x^T\\ \sigma_y^T\\ \sigma_{xy}^T\end{Bmatrix} = \begin{bmatrix}Q_{11}^T & Q_{12}^T & 0\\ Q_{12}^T & Q_{22}^T & 0\\ 0 & 0 & Q_{66}^T\end{bmatrix}\begin{Bmatrix}\varepsilon_x\\ \varepsilon_y\\ \gamma_{xy}\end{Bmatrix},\quad \begin{Bmatrix}\sigma_{yz}^T\\ \sigma_{xz}^T\end{Bmatrix} = \begin{bmatrix}Q_{44}^T & 0\\ 0 & Q_{55}^T\end{bmatrix}\begin{Bmatrix}\gamma_{yz}\\ \gamma_{xz}\end{Bmatrix}$$

$$\begin{Bmatrix}\sigma_x^C\\ \sigma_y^C\\ \sigma_{xy}^C\end{Bmatrix} = \begin{bmatrix}Q_{11}^C & Q_{12}^C & 0\\ Q_{12}^C & Q_{22}^C & 0\\ 0 & 0 & Q_{66}^C\end{bmatrix}\begin{Bmatrix}\varepsilon_x\\ \varepsilon_y\\ \gamma_{xy}\end{Bmatrix},\quad \begin{Bmatrix}\sigma_{yz}^C\\ \sigma_{xz}^C\end{Bmatrix} = \begin{bmatrix}Q_{44}^C & 0\\ 0 & Q_{55}^C\end{bmatrix}\begin{Bmatrix}\gamma_{yz}\\ \gamma_{xz}\end{Bmatrix}$$

$$\begin{Bmatrix}\sigma_x^B\\ \sigma_y^B\\ \sigma_{xy}^B\end{Bmatrix} = \begin{bmatrix}Q_{11}^T & Q_{12}^T & 0\\ Q_{12}^T & Q_{22}^T & 0\\ 0 & 0 & Q_{66}^T\end{bmatrix}\begin{Bmatrix}\varepsilon_x\\ \varepsilon_y\\ \gamma_{xy}\end{Bmatrix},\quad \begin{Bmatrix}\sigma_{yz}^B\\ \sigma_{xz}^B\end{Bmatrix} = \begin{bmatrix}Q_{44}^T & 0\\ 0 & Q_{55}^T\end{bmatrix}\begin{Bmatrix}\gamma_{yz}\\ \gamma_{xz}\end{Bmatrix} \tag{4}$$

where above index "T", "C" and "B" are Top outer skin, Core material, Bottom outer skin respectively and

$$Q_{11}^c = \frac{E_1^C}{1-v_{12}^C v_{21}^C},\quad Q_{12}^c = \frac{v_{12}^C E_2^C}{1-v_{12}^C v_{21}^C},\quad Q_{22}^c = \frac{E_2^C}{1-v_{12}^C v_{21}^C},$$

$$Q_{66}^C = G_{12}^C,\quad Q_{44}^C = G_{23}^C,\quad Q_{55}^C = G_{13}^C,\quad Q_{11}^T = Q_{22}^T = \frac{E}{1-v^2},$$

$$Q_{12}^T = \frac{vE}{1-v^2},\quad Q_{66}^T = Q_{44}^T = Q_{55}^T = \frac{E}{2(1+v)}. \tag{5}$$

The forces and moments of the double curved shallow shell can be expressed in terms of stress components across the double curved shallow shell thickness as

$$(N_i, M_i) = \int_{\frac{-h_2}{2}-h_3}^{\frac{-h_2}{2}} \sigma_i^B(1,z)dz + \int_{\frac{-h_2}{2}}^{\frac{h_2}{2}} \sigma_i^C(1,z)dz + \int_{\frac{h_2}{2}}^{\frac{h_2}{2}+h_1} \sigma_i^T(1,z)dz,$$

$$i = x, y, xy$$

$$Q_i = K\int_{\frac{-h_2}{2}-h_3}^{\frac{-h_2}{2}} \sigma_{iz}^B dz + K\int_{\frac{-h_2}{2}}^{\frac{h_2}{2}} \sigma_{iz}^C dz + K\int_{\frac{h_2}{2}}^{\frac{h_2}{2}+h_1} \sigma_{iz}^T dz, i = x, y \tag{6}$$

Substitution of Eq. (4) into Eq. (6) gives the constitutive relations as

$$\begin{aligned}
N_x &= D_1\varepsilon_x^0 + D_2\varepsilon_y^0 + D_3\varepsilon_x^1 + D_4\varepsilon_y^1,\\
N_y &= D_2\varepsilon_x^0 + D_5\varepsilon_y^0 + D_4\varepsilon_x^1 + D_6\varepsilon_y^1,\\
N_{xy} &= D_7\gamma_{xy}^0 + D_8\gamma_{xy}^1,\\
M_x &= D_3\varepsilon_x^0 + D_4\varepsilon_y^0 + D_9\varepsilon_x^1 + D_{10}\varepsilon_y^1,\\
M_y &= D_4\varepsilon_x^0 + D_6\varepsilon_y^0 + D_{10}\varepsilon_x^1 + D_{11}\varepsilon_y^1,\\
M_{xy} &= D_8\gamma_{xy}^0 + D_{12}\gamma_{xy}^1,\\
Q_x &= KD_{13}\gamma_{xz}^0,\\
Q_y &= KD_{15}\gamma_{yz}^0,
\end{aligned} \tag{7}$$

where K is correction factor, $K = \frac{5}{6}$ and

$$\begin{aligned}
D_1 &= Q_{11}^T(h_1+h_3) + Q_{11}^C h_2;\ D_2 = Q_{12}^T(h_1+h_3) + Q_{12}^C h_2,\\
D_3 &= \frac{1}{2}Q_{11}^T(h_1^2 + h_1h_2 - h_2h_3 - h_3^2)\\
D_4 &= \frac{1}{2}Q_{12}^T(h_1^2 + h_1h_2 - h_2h_3 - h_3^2);\ D_5 = Q_{22}^T(h_1+h_3) + Q_{22}^C h_2\\
D_6 &= \frac{1}{2}Q_{22}^T(h_1^2 + h_1h_2 - h_2h_3 - h_3^2);\ D_7 = Q_{66}^T(h_1+h_3) + Q_{66}^C h_2\\
D_8 &= \frac{1}{2}Q_{66}^T(h_1^2 + h_1h_2 - h_2h_3 - h_3^2)\\
D_9 &= \frac{1}{12}Q_{11}^C h_2^3 + \frac{1}{3}Q_{11}^T\left[-\frac{h_2^3}{4} + \left(\frac{h_2}{2}+h_3\right)^3 + \left(\frac{h_2}{2}+h_1\right)^3\right]\\
D_{10} &= \frac{1}{12}Q_{12}^C h_2^3 + \frac{1}{3}Q_{12}^T\left[-\frac{h_2^3}{4} + \left(\frac{h_2}{2}+h_3\right)^3 + \left(\frac{h_2}{2}+h_1\right)^3\right]\\
D_{11} &= \frac{1}{12}Q_{22}^C h_2^3 + \frac{1}{3}Q_{22}^T\left[-\frac{h_2^3}{4} + \left(\frac{h_2}{2}+h_3\right)^3 + \left(\frac{h_2}{2}+h_1\right)^3\right]\\
D_{12} &= \frac{1}{12}Q_{66}^C h_2^3 + \frac{1}{3}Q_{66}^T\left[-\frac{h_2^3}{4} + \left(\frac{h_2}{2}+h_3\right)^3 + \left(\frac{h_2}{2}+h_1\right)^3\right]\\
D_{13} &= Q_{55}^c h_2 + Q_{55}^T(h_1+h_3);\ D_{14} = \frac{1}{2}Q_{55}^T(h_1^2 + h_1h_2 - h_2h_3 - h_3^2)\\
D_{15} &= Q_{44}^c h_2 + Q_{44}^T(h_1+h_3);\ D_{16} = \frac{1}{2}Q_{44}^T(h_1^2 + h_1h_2 - h_2h_3 - h_3^2).
\end{aligned} \tag{8}$$

The reverse relations are obtained from Eq. (7)

$$\begin{cases}
\varepsilon_x^0 = -\frac{D_5}{D_2^2 - D_1D_5}N_x + \frac{D_2}{D_2^2 - D_1D_5}N_y + \frac{D_3D_5 - D_2D_4}{D_2^2 - D_1D_5}\varepsilon_x^1 + \frac{D_4D_5 - D_2D_6}{D_2^2 - D_1D_5}\varepsilon_y^1\\
\varepsilon_y^0 = \frac{D_2}{D_2^2 - D_1D_5}N_x - \frac{D_1}{D_2^2 - D_1D_5}N_y + \frac{D_1D_4 - D_2D_3}{D_2^2 - D_1D_5}\varepsilon_x^1 + \frac{D_1D_6 - D_2D_4}{D_2^2 - D_1D_5}\varepsilon_y^1\\
\gamma_{xy}^0 = \frac{1}{D_7}N_{xy} - \frac{D_8}{D_7}\gamma_{xy}^1.
\end{cases} \tag{9}$$

According to the FSDT, the equations of motion for the double curved shallow shells are [36–38]

$$\frac{\partial N_x}{\partial x} + \frac{\partial N_{xy}}{\partial y} = I_0\frac{\partial^2 u}{\partial t^2} + I_1\frac{\partial^2\phi_x}{\partial t^2}, \tag{10a}$$

$$\frac{\partial N_{xy}}{\partial x} + \frac{\partial N_y}{\partial y} = I_0\frac{\partial^2 v}{\partial t^2} + I_1\frac{\partial^2\phi_y}{\partial t^2}, \tag{10b}$$

$$\begin{aligned}
&\frac{\partial Q_x}{\partial x} + \frac{\partial Q_y}{\partial y} + N_x\frac{\partial^2 w}{\partial x^2} + 2N_{xy}\frac{\partial^2 w}{\partial x\partial y} + N_y\frac{\partial^2 w}{\partial y^2} - K_1 w\\
&\quad + K_2\left(\frac{\partial^2 w}{\partial x^2} + \frac{\partial^2 w}{\partial y^2}\right) + p(t) + \frac{N_x}{R_x} + \frac{N_y}{R_y} = I_0\frac{\partial^2 w}{\partial t^2} + 2\varepsilon I_0\frac{\partial w}{\partial t},
\end{aligned} \tag{10c}$$

$$\frac{\partial M_x}{\partial x} + \frac{\partial M_{xy}}{\partial y} - Q_x = I_1\frac{\partial^2 u}{\partial t^2} + I_2\frac{\partial^2\phi_x}{\partial t^2}, \tag{10d}$$

$$\frac{\partial M_{xy}}{\partial x} + \frac{\partial M_y}{\partial y} - Q_y = I_1\frac{\partial^2 v}{\partial t^2} + I_2\frac{\partial^2\phi_y}{\partial t^2}, \tag{10e}$$

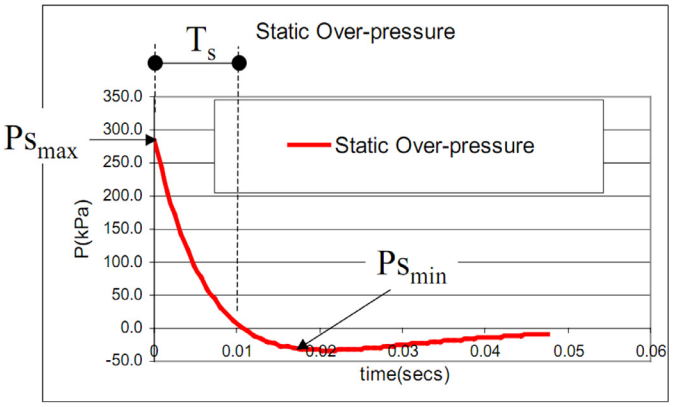

Fig. 4. Blast pressure function.

where ε is damping coefficient [36,37]:

$$I_i = \int_{-\frac{h_2}{2}-h_3}^{-\frac{h_2}{2}} \rho^B z^i dz + \int_{-\frac{h_2}{2}}^{\frac{h_2}{2}} \rho^c z^i dz + \int_{\frac{h_2}{2}}^{\frac{h_2}{2}+h_1} \rho^T z^i dz, (i = 0,1,2). \tag{11}$$

The blast load $p(t)$ is a short-term load and generated by an explosion or by a shock-wave disturbance produced by an aircraft flying at supersonic speed, or by a supersonic projectile, rocket or missile operating in its vicinity. It can be expressed as [24] and shown by the example presented in Fig. 4.

$$p(t) = 1.8Ps_{max}\left(1 - \frac{t}{T_s}\right)exp\left(\frac{-bt}{T_s}\right), \tag{12}$$

where the "1.8" factor accounts for the effects of a hemispherical blast, $P\,s_{max}$ is the maximum (or peak) static over-pressure, b is the parameter controlling the rate of wave amplitude decay and T_s is the parameter characterizing the duration of the blast pulse.

The stress function $f(x, y, t)$ is introduced as

$$N_x = \frac{\partial^2 f}{\partial y^2}, N_y = \frac{\partial^2 f}{\partial x^2}, N_{xy} = -\frac{\partial^2 f}{\partial x\partial y}. \tag{13}$$

Replacing Eq. (13) into Eq. (10a) and (10b) yields

$$\frac{\partial^2 u}{\partial t^2} = -\frac{I_1}{I_0}\frac{\partial^2\phi_x}{\partial t^2}, \tag{14a}$$

$$\frac{\partial^2 v}{\partial t^2} = -\frac{I_1}{I_0}\frac{\partial^2\phi_y}{\partial t^2}. \tag{14b}$$

By substituting Eq. (14a) and (b) into Eq. (10c–e), Eq. (10c–e) can be rewritten

$$\begin{aligned}
&\frac{\partial Q_x}{\partial x} + \frac{\partial Q_y}{\partial y} + \frac{\partial^2 f}{\partial y^2}\frac{\partial^2 w}{\partial x^2} - 2\frac{\partial^2 f}{\partial x\partial y}\frac{\partial^2 w}{\partial x\partial y} + \frac{\partial^2 f}{\partial x^2}\frac{\partial^2 w}{\partial y^2} - K_1 w\\
&\quad + K_2\left(\frac{\partial^2 w}{\partial x^2} + \frac{\partial^2 w}{\partial y^2}\right) + p(t) + \frac{1}{R_x}\frac{\partial^2 f}{\partial y^2} + \frac{1}{R_y}\frac{\partial^2 f}{\partial x^2}\\
&= I_0\frac{\partial^2 w}{\partial t^2} + 2\varepsilon I_0\frac{\partial w}{\partial t},
\end{aligned} \tag{15a}$$

$$\frac{\partial M_x}{\partial x} + \frac{\partial M_{xy}}{\partial y} - Q_x = \left(I_2 - \frac{I_1^2}{I_0}\right)\frac{\partial^2\phi_x}{\partial t^2}, \tag{15b}$$

$$\frac{\partial M_{xy}}{\partial x} + \frac{\partial M_y}{\partial y} - Q_y = \left(I_2 - \frac{I_1^2}{I_0}\right)\frac{\partial^2\phi_y}{\partial t^2}. \tag{15c}$$

By substituting Eq. (9) into Eq. (7) and then into Eq. (15), the system of motion Eq. (15) is rewritten as follows

$$H_{11}(w) + H_{12}(\phi_x) + H_{13}(\phi_y) + P(w,f) + p(t) = I_0\frac{\partial^2 w}{\partial t^2} + 2\varepsilon I_0\frac{\partial w}{\partial t}, \tag{16a}$$

$$H_{21}(w)+H_{22}(\phi_x)+H_{23}(\phi_y)+H_{24}(f)=\left(I_2-\frac{I_1^2}{I_0}\right)\frac{\partial^2\phi_x}{\partial t^2}, \tag{16b}$$

$$H_{31}(w)+H_{32}(\phi_x)+H_{33}(\phi_y)+H_{34}(f)=\left(I_2-\frac{I_1^2}{I_0}\right)\frac{\partial^2\phi_y}{\partial t^2}. \tag{16c}$$

where

$$\begin{aligned}
H_{11}(w) &= KD_{13}\frac{\partial^2 w}{\partial x^2}+KD_{15}\frac{\partial^2 w}{\partial y^2}-K_1 w+K_2\left(\frac{\partial^2 w}{\partial x^2}+\frac{\partial^2 w}{\partial y^2}\right),\\
H_{12}(\phi_x) &= KD_{13}\frac{\partial\phi_x}{\partial x},\ H_{13}(\phi_y)=KD_{15}\frac{\partial\phi_y}{\partial y},\\
P(w,f) &= \frac{\partial^2 f}{\partial y^2}\frac{\partial^2 w}{\partial x^2}-2\frac{\partial^2 f}{\partial x\partial y}\frac{\partial^2 w}{\partial x\partial y}+\frac{\partial^2 f}{\partial x^2}\frac{\partial^2 w}{\partial y^2}+\frac{1}{R_y}\frac{\partial^2 f}{\partial x^2}+\frac{1}{R_x}\frac{\partial^2 f}{\partial y^2},\\
H_{21}(w) &= -KD_{13}\frac{\partial w}{\partial x},\\
H_{22}(\phi_x) &= \left(\frac{D_3^2D_5-2D_2D_3D_4+D_1D_4^2}{D_2^2-D_1D_5}+C_9\right)\frac{\partial^2\phi_x}{\partial x^2}\\
&\quad+\left(D_{12}-\frac{D_8^2}{D_7}\right)\frac{\partial^2\phi_x}{\partial y^2}-KD_{13}\phi_x,\\
H_{23}(\phi_y) &= \left(\frac{D_3(D_4D_5-D_6D_2)+D_4(D_1D_6-D_2D_4)}{D_2^2-D_1D_5}\right.\\
&\quad\left.+D_{10}+D_{12}-\frac{D_8^2}{D_7}\right)\frac{\partial^2\phi_y}{\partial x\partial y},\\
H_{24}(f) &= \left(\frac{D_2D_4-D_3D_5}{D_2^2-D_1D_5}-\frac{D_8}{D_7}\right)\frac{\partial^3 f}{\partial x\partial y^2}+\frac{D_2D_3-D_1D_4}{D_2^2-D_1D_5}\frac{\partial^3 f}{\partial x^3},\\
H_{31}(w) &= -KD_{15}\frac{\partial w}{\partial y},\\
H_{32}(\phi_x) &= \left(\frac{D_4(D_3D_5-D_4D_2)+D_6(D_1D_4-D_2D_3)}{D_2^2-D_1D_5}+D_{10}\right.\\
&\quad\left.+D_{12}-\frac{D_8^2}{D_7}\right)\frac{\partial^2\phi_x}{\partial x\partial y},\\
H_{33}(\phi_y) &= \left(\frac{D_4(D_4D_5-D_6D_2)+D_6(D_1D_6-D_2D_4)}{D_2^2-D_1D_5}+D_{11}\right)\frac{\partial^2\phi_y}{\partial y^2}\\
&\quad+\left(D_{12}-\frac{D_8^2}{D_7}\right)\frac{\partial^2\phi_y}{\partial x^2}-KD_{15}\phi_y,\\
H_{34}(f) &= \left(\frac{D_2D_4-D_1D_6}{D_2^2-D_1D_5}-\frac{D_8}{D_7}\right)\frac{\partial^3 f}{\partial x^2\partial y}+\left(\frac{D_2D_6-D_4D_5}{D_2^2-D_1D_5}\right)\frac{\partial^3 f}{\partial y^3}.
\end{aligned}$$

The strains are related to the compatibility equation [35-37]:

$$\frac{\partial^2\varepsilon_x^0}{\partial y^2}+\frac{\partial^2\varepsilon_y^0}{\partial x^2}-\frac{\partial^2\gamma_{xy}^0}{\partial x\partial y}=\left(\frac{\partial^2 w}{\partial x\partial y}\right)^2-\frac{\partial^2 w}{\partial x^2}\frac{\partial^2 w}{\partial y^2}-\frac{1}{R_x}\frac{\partial^2 w}{\partial y^2}-\frac{1}{R_y}\frac{\partial^2 w}{\partial x^2}. \tag{17}$$

Set Eqs. (13) and (9) into the deformation compatibility Eq. (17), we obtain

$$\begin{aligned}
&-A_{11}\frac{\partial^4 f}{\partial x^4}-A_{12}\frac{\partial^4 f}{\partial y^4}+A_{13}\frac{\partial^4 f}{\partial x^2\partial y^2}+A_{21}\frac{\partial^3\phi_x}{\partial x^3}+A_{22}\frac{\partial^3\phi_y}{\partial y^3}\\
&+A_{23}\frac{\partial^3\phi_x}{\partial x\partial y^2}+A_{24}\frac{\partial^3\phi_y}{\partial x^2\partial y}\\
&-\left(\left(\frac{\partial^2 w}{\partial x\partial y}\right)^2-\frac{\partial^2 w}{\partial x^2}\frac{\partial^2 w}{\partial y^2}-\frac{1}{R_x}\frac{\partial^2 w}{\partial y^2}-\frac{1}{R_y}\frac{\partial^2 w}{\partial x^2}\right)=0
\end{aligned} \tag{18}$$

where

$$\begin{aligned}
A_{11} &= \frac{D_1}{D_2^2-D_1D_5},\ A_{12}=\frac{D_5}{D_2^2-D_1D_5},\ A_{13}=\frac{2D_2}{D_2^2-D_1D_5}+\frac{1}{D_7},\\
A_{21} &= \frac{D_1D_4-D_2D_3}{D_2^2-D_1D_5},\ A_{22}=\frac{D_4D_5-D_6D_2}{D_2^2-D_1D_5},\ A_{23}=\frac{D_3D_5-D_4D_2}{D_2^2-D_1D_5}+\frac{D_8}{D_7},\\
A_{24} &= \frac{D_1D_6-D_2D_4}{D_2^2-D_1D_5}+\frac{D_8}{D_7}.
\end{aligned} \tag{19}$$

Eqs. (16a–c) and (18) are nonlinear equations in terms of variables w, φ_x, φ_y and f and are used to investigate the nonlinear vibration and dynamic stability of the double curved shallow shell with negative Poisson's ratio in auxetic honeycombs core layer using the FSDT.

3.2. Nonlinear dynamical analysis

Considering the following boundary condition: four edges of double curved shallow shell are simply supported; immovable edge is under blast load $p(t)$. Thus, the boundary conditions are [7,36,37]

$$\begin{aligned}
&w=N_{xy}=\phi_y=M_x=0, N_x=N_{x0}\ \text{at}\ x=0\ \text{and}\ x=a\\
&w=N_{xy}=\phi_y=M_y=0, N_y=N_{y0}\ \text{at}\ =0\ \text{and}\ y=a
\end{aligned} \tag{20}$$

in which N_{x0}, N_{y0} are the forces acting on the edges of the double curved shallow shells.

The approximate solutions of the system of Eqs. (16a and c) and (18) satisfying the boundary condition (20) can be written as

$$\begin{aligned}
w(x,y,t) &= W(t)\sin\alpha x\sin\beta y,\\
\phi_x(x,y,t) &= \Phi_x(t)\cos\alpha x\sin\beta y,\\
\phi_y(x,y,t) &= \Phi_y(t)\sin\alpha x\cos\beta y,\\
(x,y,t) &= A_1(t)\cos 2\alpha x+A_2(t)\cos 2\beta y+A_3(t)\sin\alpha x\sin\beta y\\
&\quad+\frac{1}{2}N_{x0}y^2+\frac{1}{2}N_{y0}x^2
\end{aligned} \tag{21}$$

where $\alpha=\frac{m\pi}{a}, \beta=\frac{n\pi}{b}, m,n=1,2\ldots$ are the natural numbers of half waves in the corresponding direction x, y and W, Φ_x, Φ_y the amplitudes which are functional dependent on time.

The coefficients $A_i=(1\div 3)$ are determined by substitution of Eq. (21) into Eq. (18) as

$$\begin{aligned}
A_1 &= \frac{\left(D_1D_5-D_2^2\right)}{32D_1}\frac{\beta^2}{\alpha^2}W^2(t),\quad A_2=\frac{\left(D_1D_5-D_2^2\right)}{32D_5}\frac{\alpha^2}{\beta^2}W^2(t),\\
A_3 &= a_1\Phi_x(t)+a_2\Phi_y(t)-a_3W(t),
\end{aligned} \tag{22}$$

where

$$\begin{aligned}
a_1 &= \frac{\left[\left(\frac{D_1D_4-D_2D_3}{D_2^2-D_1D_5}\right)\alpha^3+\left(\frac{D_3D_5-D_4D_2}{D_2^2-D_1D_5}+\frac{D_8}{D_7}\right)\alpha\beta^2\right]}{\frac{D_1}{D_2^2-D_1D_5}\alpha^4+\frac{D_5}{D_2^2-D_1D_5}\beta^4-\left(\frac{2D_2}{D_2^2-D_1D_5}+\frac{1}{D_7}\right)\alpha^2\beta^2}\\
a_2 &= \frac{\left[\left(\frac{D_4D_5-D_6D_2}{D_2^2-D_1D_5}\right)\beta^3+\left(\frac{D_1D_6-D_2D_4}{D_2^2-D_1D_5}+\frac{D_8}{D_7}\right)\alpha^2\beta\right]}{\frac{D_1}{D_2^2-D_1D_5}\alpha^4+\frac{D_5}{D_2^2-D_1D_5}\beta^4-\left(\frac{2D_2}{D_2^2-D_1D_5}+\frac{1}{D_7}\right)\alpha^2\beta^2}\\
a_3 &= \frac{1}{\frac{D_1}{D_2^2-D_1D_5}\alpha^4+\frac{D_5}{D_2^2-D_1D_5}\beta^4-\left(\frac{2D_2}{D_2^2-D_1D_5}+\frac{1}{D_7}\right)\alpha^2\beta^2}\left(\frac{\beta^2}{R_x}+\frac{\alpha^2}{R_y}\right).
\end{aligned}$$

Replacing Eq. (21) into the equations of motion (16a)–(16c) and then applying Galerkin method, we obtain

$$\begin{aligned}
&h_{11}W+h_{12}\Phi_x+h_{13}\Phi_y+h_{14}W^3+h_{15}\Phi_xW\\
&+h_{16}\Phi_yW+h_{17}W^2+q\frac{4ab}{mn\pi^2}=\frac{ab}{4}\left(I_0\frac{\partial^2 w}{\partial t^2}+2\varepsilon I_0\frac{\partial w}{\partial t}\right),
\end{aligned} \tag{23a}$$

$$h_{21}W+h_{22}\Phi_x+h_{23}\Phi_y+h_{24}W^2=\left(I_2-\frac{I_1^2}{I_0}\right)\frac{ab}{4}\frac{\partial^2\Phi_x}{\partial t^2}, \tag{23b}$$

$$h_{31}W+h_{32}\Phi_x+h_{33}\Phi_y+h_{34}W^2=\left(I_2-\frac{I_1^2}{I_0}\right)\frac{ab}{4}\frac{\partial^2\Phi_y}{\partial t^2}. \tag{23c}$$

where

$$h_{11} = [-\alpha^2 K D_{13} - \beta^2 K D_{15} - K_1 - K_2(\alpha^2+\beta^2) - \alpha^2 N_{x0} - \beta^2 N_{y0}]\frac{ab}{4} + a_3\left(\frac{1}{R_x}\beta^2 + \frac{1}{R_y}\alpha^2\right)\frac{ab}{4},$$

$$h_{12} = -\alpha K D_{13}\frac{ab}{4} + a_1\left(\frac{1}{R_x}\beta^2 + \frac{1}{R_y}\alpha^2\right)\frac{ab}{4};$$

$$h_{13} = -\beta K D_{15}\frac{ab}{4} + a_2\left(\frac{1}{R_x}\beta^2 + \frac{1}{R_y}\alpha^2\right)\frac{ab}{4},$$

$$h_{14} = -\alpha^4\frac{D_1D_5 - D_2^2}{32D_5}\frac{ab}{2} - \beta^4\frac{D_1D_5 - D_2^2}{32D_1}\frac{ab}{2},$$

$$h_{15} = a_1\frac{8mn\pi^2}{3ab}, h_{16} = a_2\frac{8mn\pi^2}{3ab}, h_{17} = -a_3\frac{8mn\pi^2}{3ab}$$

$$h_{18} = -\alpha^2 N_{x0}\frac{ab}{4} - \beta^2 N_{y0}\frac{ab}{4} - K D_7(\alpha^2+\beta^2)\frac{ab}{4},$$

$$h_{21} = -\alpha K D_{13}\frac{ab}{4} + \left[\alpha\beta^2\left(\frac{D_2D_4 - D_3D_5}{D_2^2 - D_1D_5} - \frac{D_8}{D_7}\right) + \alpha^3\left(\frac{D_2D_3 - D_1D_4}{D_2^2 - D_1D_5}\right)\right]\frac{ab}{4}a_3,$$

$$h_{22} = \left[-\alpha^2\left(\frac{D_3^2D_5 - 2D_2D_3D_4 + D_1D_4^2}{D_2^2 - D_1D_5} + D_9\right) - \beta^2\left(D_{12} - \frac{D_8^2}{D_7}\right) - K D_{13}\right]\frac{ab}{4} + \left[-\alpha\beta^2\left(\frac{D_2D_4 - D_3D_5}{D_2^2 - D_1D_5} - \frac{D_8}{D_7}\right) - \alpha^3\left(\frac{D_2D_3 - D_1D_4}{D_2^2 - D_1D_5}\right)\right]\frac{ab}{4}a_1,$$

$$h_{23} = -\alpha\beta\left(\frac{D_3(D_4D_5 - D_6D_2) + D_4(D_1D_6 - D_2D_4)}{D_2^2 - D_1D_5} + D_{10} + D_{12} - \frac{D_8^2}{D_7}\right)\frac{ab}{4} + \left[-\alpha\beta^2\left(\frac{D_2C_4 - D_3D_5}{D_2^2 - D_1D_5} - \frac{D_8}{D_7}\right) - \alpha^3\left(\frac{D_2D_3 - D_1D_4}{D_2^2 - D_1D_5}\right)\right]\frac{ab}{4}a_2,$$

$$h_{24} = 8\alpha^3\frac{D_2D_3 - D_1D_4}{D_2^2 - D_1D_5}\frac{8ab}{3mn\pi^2}\frac{D_1D_5 - D_2^2}{32D_1}\frac{\beta^2}{\alpha^2},$$

$$h_{31} = -\beta K D_{15}\frac{ab}{4} + \left[\left(\frac{D_2D_4 - D_1D_6}{D_2^2 - D_1D_5} - \frac{D_8}{D_7}\right)\alpha^2\beta + \left(\frac{D_2D_6 - D_4D_5}{D_2^2 - D_1D_5}\right)\beta^3\right]\frac{ab}{4}a_3,$$

$$h_{32} = -\alpha\beta\left(\frac{D_4(D_3D_5 - D_4D_2) + D_6(D_1D_4 - D_2D_3)}{D_2^2 - D_1D_5} + D_{10} + D_{12} - \frac{D_8^2}{D_7}\right)\frac{ab}{4}, - \left[\left(\frac{D_2D_4 - D_1D_6}{D_2^2 - D_1D_5} - \frac{D_8}{D_7}\right)\alpha^2\beta + \left(\frac{D_2D_6 - D_4D_5}{D_2^2 - D_1D_5}\right)\beta^3\right]\frac{ab}{4}a_1,$$

$$h_{33} = \left[-\left(\frac{D_4(D_4D_5 - D_6D_2) + D_6(D_1D_6 - D_2D_4)}{D_2^2 - D_1D_5} + D_{11}\right)\beta^2 - \left(D_{12} - \frac{D_8^2}{D_7}\right)\alpha^2 - K D_{15}\right]\frac{ab}{4} - \left[\left(\frac{D_2D_4 - D_1D_6}{D_2^2 - D_1D_5} - \frac{D_8}{D_7}\right)\alpha^2\beta + \left(\frac{D_2D_6 - D_4D_5}{D_2^2 - D_1D_5}\right)\beta^3\right]\frac{ab}{4}a_2,$$

$$h_{34} = 8\beta^3\frac{D_2D_6 - D_4D_5}{D_2^2 - D_1D_5}\frac{8ab}{3mn\pi^2}\frac{D_1D_5 - D_2^2}{32D_5}\frac{\alpha^2}{\beta^2}.$$

The Eq. (23a–c) are basic equations to determine nonlinear dynamic response and vibration of the shells with negative Poisson's ratios in auxetic honeycombs core layer using FSDT. It is solved by using the fourth-order Runge–Kutta method.

Taking linear parts of the set of Eq. (23), the natural frequencies of the shell can be determined directly by solving determinant

$$\begin{vmatrix} h_{11} + I_0\omega^2 & h_{12} & h_{13} \\ h_{21} & h_{22} + \rho_1\omega^2 & h_{23} \\ h_{31} & h_{32} & h_{33} + \rho_1\omega^2 \end{vmatrix} = 0. \quad (24)$$

Solving Eq. (24) yields three angular frequencies, the smallest one is being considered.

4. Numerical results and discussion

The parameters for the geometric parameters of double curved shallow shell with negative Poisson's ratio were chosen as below

$$R_x = R_y = 6m, h_1 = h_3 = 0.00667m, h_2 = 0.02m,$$

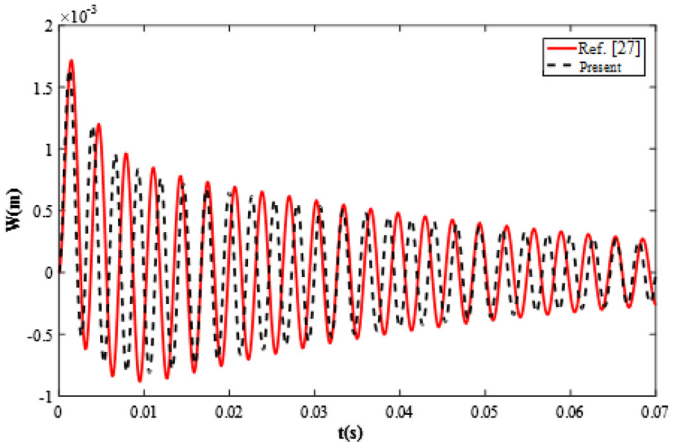

Fig. 5. Comparison of nonlinear dynamic response of the plate on elastic foundations subjected to blast load with results of Duc et al. [27].

$$h = h_1 + h_2 + h_3, a/h = 30, a = b, m = n = 1,$$
$$t/l = 0.0138571, h/l = 2, \theta = -55^o, E = 70GPa,$$
$$G = 26GPa, \rho = 2702kg/m^3, \nu = 0.33,$$

4.1. Numerical verification

To evaluate the reliability of the method used in the paper, we have made a comparison of the results of the study [27]. If we choose $R_x \to \infty$, $R_y \to \infty$, the nonlinear dynamic response of the double curved shallow shell will turn into the nonlinear dynamic response of plate. Fig. 5 shows the comparison between the obtained result using present method for the nonlinear dynamic response of plate only made of ceramic ($N = 0$) on the elastic foundations subjected to blast load and the result of Duc et al. [27]. In [27], the authors investigated the nonlinear dynamic response vibration of FGM plates on elastic foundations subjected to blast with the volume fraction index taken $N = 0$. From Fig. 5, it can be seen that a good agreement is obtained in this comparison.

The geometry parameters and material parameters in the Fig. 5 are chosen as follows

$$N = 0, m = n = 1, b/a = 1, b/h = 20, K_1 = 0.3\,GPa/m, K_2 = 0.02\,GPa.m,$$
$$E_1^c = E_2^c = E = 384.43 \times 10^9 Pa, G_{12}^c = G_{13}^c = G_{23}^c = G = \frac{E}{2(1+\upsilon)},$$
$$\rho = \rho_c = 2370\,kg/m^3.$$

4.2. Nonlinear dynamic response

Effects of elastic foundations on the natural frequency of the composite double curved shallow shells with negative Poisson's ratio in auxetic honeycombs are shown in Table 2. The value of the natural frequency increases when the values K_1 and K_2 increase. Table 2 also shows that the lowest natural frequency corresponds to mode $(m, n) = (1, 1)$.

Figs. 6 and 7 show the effects of the elastic foundations (linear Winkler foundation and Pasternak foundation) on the nonlinear dynamic response of auxetic material of double curved shallow shell with negative Poisson's ratio under blast load ($\nu_{12} = -0.3401$). From the figures, it can be seen that the elastic foundations make the vibration amplitude of the auxetic material of double curvature shell with negative Poisson's ratio reduce when increasing the coefficients of elastic foundations (K_1 and K_2). That shows the positive effect of elastic foundations. Furthermore, Winkler's elastic foundation (K_1) is weaker than Pasternak's foundation (K_2).

Fig. 8 shows the influence of ratio $a/h = (10, 20, 30)$ on nonlinear dynamic response of the auxetic material of the double curved shallow shell with negative Poisson's ratio under blast load($\nu_{12} = -0.3401$).

Table 2
Effect of elastic foundations on natural frequencies (s^{-1}) of the composite double curved shallow shells with negative Poisson's ratio in auxetic honeycombs with $\nu_{12} = -0.3401$.

		$K_2 = 0$	$K_2 = 0.02$ GPam	$K_2 = 0.04$ GPam
$(m, n) = (1, 1)$	$K_1 = 0$	5690	6531	7276
	$K_1 = 0.3\ GPa/m$	6340	7105	7795
	$K_1 = 0.5\ GPa/m$	6730	7463	8123
$(m, n) = (1, 3)$	$K_1 = 0$	25,401	26,394	27,351
	$K_1 = 0.3\ GPa/m$	25,554	26,542	27,493
	$K_1 = 0.5\ GPa/m$	25,656	26,640	27,588
$(m, n) = (1, 5)$	$K_1 = 0$	43,530	45,040	46,501
	$K_1 = 0.3\ GPa/m$	43,620	45,127	46,585
	$K_1 = 0.5\ GPa/m$	43,680	45,184	46,640
$(m, n) = (3, 5)$	$K_1 = 0$	39,431	41,549	43,565
	$K_1 = 0.3\ GPa/m$	39,528	41,642	43,653
	$K_1 = 0.5\ GPa/m$	39,593	41,703	43,711
$(m, n) = (5, 5)$	$K_1 = 0$	37,021	40,217	43,176
	$K_1 = 0.3\ GPa/m$	37,123	40,310	43,262
	$K_1 = 0.5\ GPa/m$	37,190	40,372	43,320
$(m, n) = (7, 5)$	$K_1 = 0$	42,447	46,490	50,206
	$K_1 = 0.3\ GPa/m$	42,534	46,570	50,280
	$K_1 = 0.5\ GPa/m$	42,592	46,622	50,329

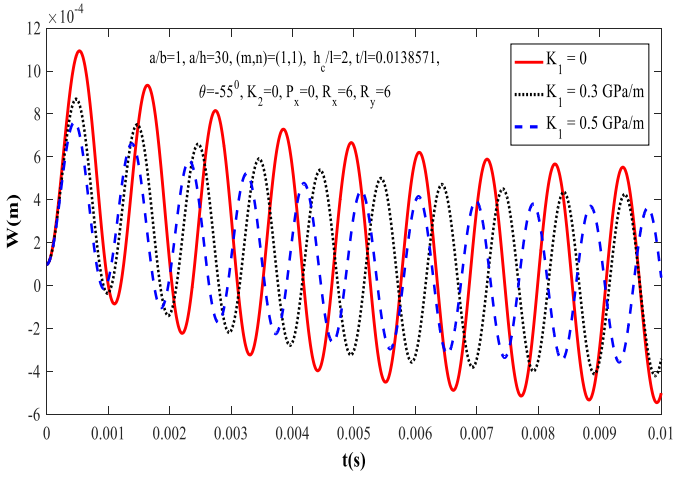

Fig. 6. Effect of the linear Winkler foundation on the nonlinear dynamic response of the shell under blast load.

From Fig. 8, we can see that when a/h is increased, the curve becomes higher and vice versa. This is correct because when a/h is increased, the sandwich plates becomes thinner and the load capacity is decreased.

Fig. 9 shows the influence of ratio $a/b = (0.5, 1, 2)$ on the nonlinear dynamic response of the auxetic material of the double curved shallow shell with negative Poisson's ratio under blast load a/b. From Fig. 9, we can see that when a/b is decreased, the curve becomes lower and vice versa.

Fig. 10 shows the effect of pre-loaded axial compression P_x on the nonlinear dynamic response($\nu_{12} = -0.3401$). This figure also indicates that the nonlinear dynamic response amplitude of the auxetic material of the double curved shallow shell with auxetic core increases when the value of the pre-loaded compressive force P_x increases.

Fig. 11 shows the effect of parameter characterizing the duration of the blast pulse on nonlinear response of auxetic material of the double curved shallow shell with auxetic core with three values of $T_s = (0.005, 0.01, 0.02)$s. From the figure, it can be seen that when the value of T_s is increased, the amplitude of nonlinear response increase and vice versa. At the same time, the time from $t = 0$ to amplitude of nonlinear response unchanged increases and vice versa.

Fig. 12 illustrates the effect of damping on amplitude–time curves for nonlinear dynamic response of the double curved shallow shell with negative Poisson's ratio in core layer with three values of damping

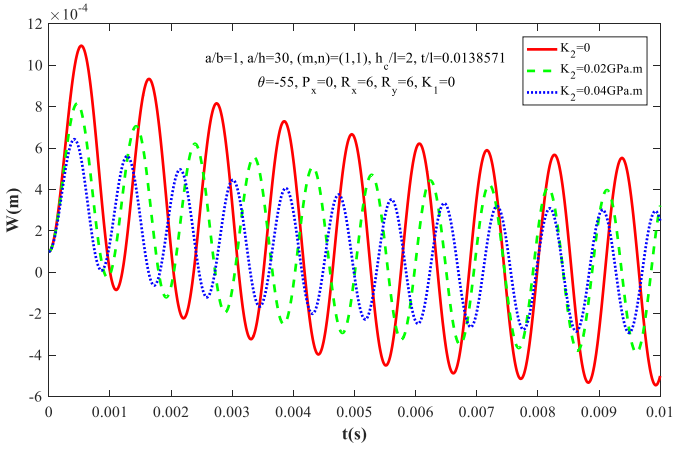

Fig. 7. Effect of the Pasternak foundation on the nonlinear dynamic response of the shell under blast load.

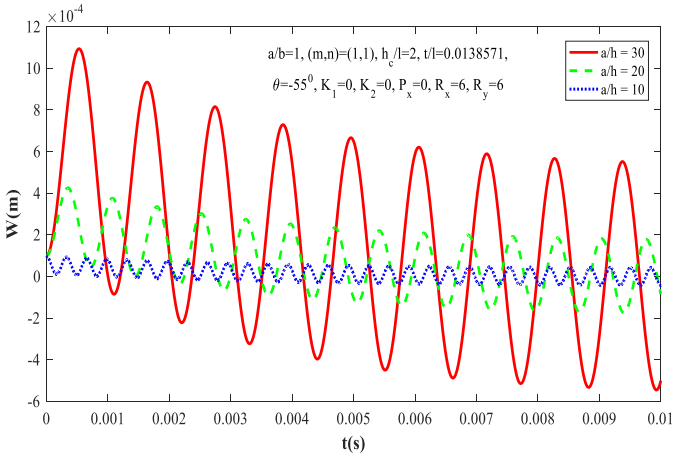

Fig. 8. Effects of ratio a/h on the nonlinear dynamic response of the shell under blast load.

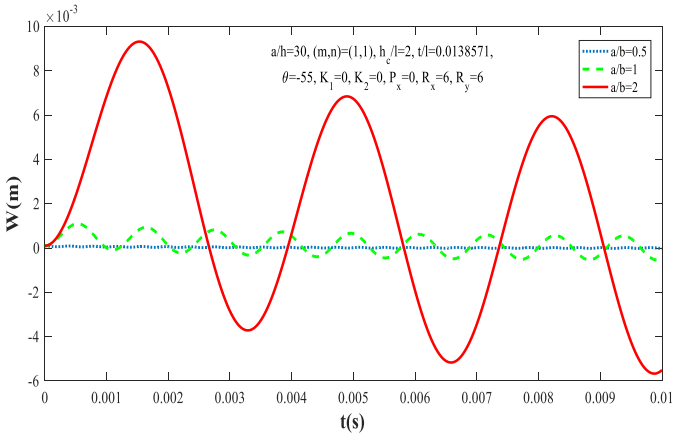

Fig. 9. Effects of ratio a/b on the nonlinear dynamic response of the shell under blast load.

coefficient $\varepsilon = (0.1, 5, 8)$. From Fig. 12, we can see that when damping coefficient ε is increased, the curve becomes lower and vice versa.

5. Conclusions

The novelty and most significant contribution of this paper is that for the first time we use analytical solution for the investigation of the

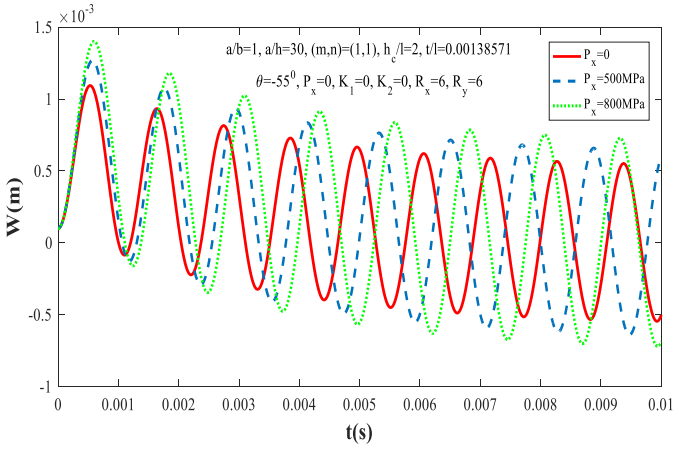

Fig. 10. Effect of pre-loaded axial P_x compression on nonlinear response of the shell under blast load.

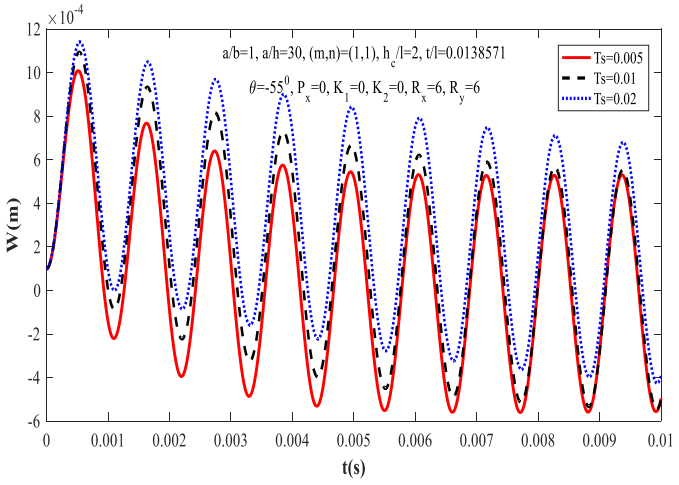

Fig. 11. Effect of parameter characterizing the duration of the blast pulse (T_s) compression on nonlinear response of the shell.

nonlinear dynamic response and vibration of composite double curved shallow shells with negative Poisson's ratios in auxetic honeycombs.

Using first order shear deformation shell theory, Galerkin method and Runge–Kutta method, the paper analyzes and discusses the effects of material and geometrical properties, elastic foundations, auxetic core layer, blast and damping loads on the nonlinear dynamic response of the composite shells. The most important finding is that the dynamic response and natural frequency of the shells could be explicitly represented in these input parameters. As a result, we are able to design a suitable auxetic composite structure under the blast and other mechanical loads.

Funding

This research is funded by Vietnam National Foundation for Science and Technology Development (NAFOSTED) under grant number 107.02-2015.03. The authors are grateful for this support.

References

[1] Love AEH. A treatise on the mathematical theory of elasticity, 1st paperback ed. Cambridge University Press, Cambridge, 1892.
[2] Voigt W. Bestimmung der Elasticitätsconstanten für das chlorsaure natron. Annalen Phys Chem 1893;285:719–23.
[3] Qiao JX, Chen CQ. Impact resistance of uniform and functionally graded auxetic double arrowhead honeycombs. Int J Impact Eng 2015;83:47–58.
[4] Lu Z, Wang Q, Li X, Yang Z. Elastic properties of two novel auxetic 3D cellular structures. Int J Solids Struct 2016. doi:10.1016/j.ijsolstr.2017.05.031.

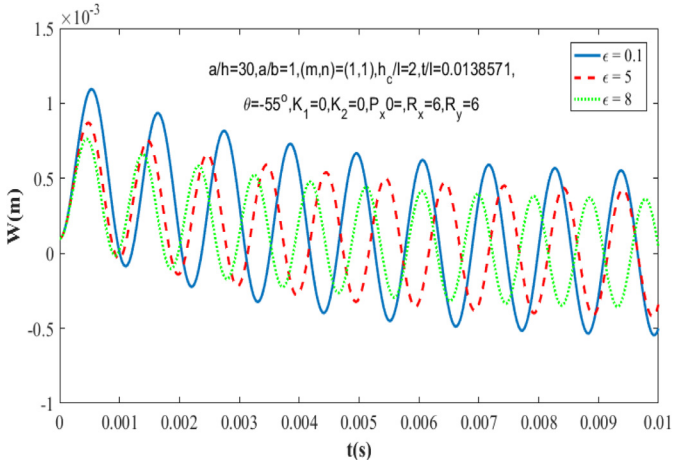

Fig. 12. Effects of damping coefficient ϵ on the nonlinear dynamic response of the auxetic material of the shell under blast load.

[5] Kwon K, Phan AV. Symmetric-Galerkin boundary element analysis of the dynamic T-stress for the interaction of a crack with an auxetic inclusion. Mech Res Commun 2015;69:91–6.
[6] Assidi M, Ganghoffer JF. Composites with auxetic inclusions showing both an auxetic behavior and enhancement of their mechanical properties. Compos Struct 2012;94:2373–82.
[7] Bhullar SK, Wegner JL, Mioduchowski A. Auxetic behavior of a thermoelastic layered plate. J Eng Technol Res 2010;2(9):161–7.
[8] Burlayenko VN, Sadowski T. Effective elastic properties of foam-filled honeycomb cores of sandwich panels. Compos Struct 2010;92:2890–900.
[9] Grima JN, Oliveri L, Attard D, Ellul B, Gatt R, Cicala G, et al. Hexagonal honeycombs with zero Poisson's ratios and enhances stiffness. Adv Eng Mater 2010;12(9):855–62.
[10] Milton GW. Composite materials with Poisson's ratios close to -1. J Mech Phys Solids 1992;40:1105–37.
[11] Yang DU, Lee S, Huang FY. Geometric effects on micropolar elastic honeycomb structure with negative Poisson's ratio using the finite element method. Finite Elem Anal Des 2003;39:187–205.
[12] Prawoto Y. Seeing auxetic materials from the mechanics point of view: a structural review on the negative Poisson's ratio. Comput Mater Sci 2012;58:140–53.
[13] Liu XF, Wang YF, Wang YS, Zhang C. Wave propagation in a sandwich plate with a periodic composite core. J Sandwich Struct Mater 2014;16(3):319–38.
[14] Jopek H, Strek T. Thermal and structural dependence of auxetic properties of composite materials. Phys Status Solidi B 2015;252(7):1551–8.
[15] Wan H, Ohtaki H, Kotosaka S, Hu G. A study of negative Poisson's ratios in auxetic honeycombs based on a large deflection model. Eur J Mech 2014;23:95–106.
[16] Grujicic M, Galgalikar R, Snipes JS, Yavari R, Ramaswami S. Multi-physics modeling of the fabrication and dynamic performance of all-metal auxetic-hexagonal sandwich-structures. Mater Des 2013;51:113–30.
[17] Qing-Tian D, Zhi-Chun Y. Wave propagation in sandwich panel with auxetic core. J Solid Mech 2010;2(4):393–402.
[18] Cielecka I, Jędrysiak J. A non-asymptotic model of dynamics of honeycomb lattice–type plates. J Sound Vib 2006;296:130–49.
[19] Lewiński T. Physical correctness of Cosserat type models of honeycomb grid plates. Theor Appl Mech 1985;23:53–69.
[20] Wierzbicki E, Woźniak C. On the dynamic behaviour of honeycomb based composite solids. Acta Mech 2000;141:161–72.
[21] Imbalzano G, Phuong T, Tuan ND, Perter V, Lee S. A numerical study of auxetic composite panels under blast loadings. Compos Struct 2016;135:339–52.
[22] Imbalzano G, Linforth S, Tuan ND, Lee PVS, Phuong T. Blast resistance of auxetic and honeycomb sandwich panels: comparisons and parametric designs. Compos Struct 2017. https://doi.org/10.1016/j.compstruct.2017.03.018.
[23] Li S, Li X, Wang Z, Wu G, Lu G, Zhao L. Finite element analysis of sandwich panels with stepwise graded aluminum honeycomb cores under blast loading. Int J Mech Sci 2015;96-97:1–12.
[24] Lam N, Mendis P, Tuan ND. Response spectrum solutions for blast loading. Electron J Struct Eng 2004;4:28–44.
[25] Qi C, Yang S, Yang LJ, Han SH, Lu ZH. Dynamic response and optimal design of curved metallic sandwich panels under blast loading. Sci World J 2014. doi:10.1155/2014/853681.
[26] Schenk M, Guest SD, McShane GJ. Novel stacked folded cores for blast-resistant sandwich beams. Int J Solids Struct 2014;51:4196–214.
[27] Duc ND, Tuan ND, Phuong T, Quan TQ. Nonlinear dynamic response and vibration of imperfect shear deformable functionally graded plates subjected to blast and thermal loads. J Mech Adv Mater Struct 2017;24(4):318–29.
[28] Tan KT, Huang HH, Sun CT. Blast-wave impact mitigation using negative effective mass density concept of elastic metamaterials. Int J Impact Eng 2014;64:20–9.
[29] Duc ND, Cong PH. Nonlinear dynamic response and vibration of sandwich composite plates with negative Poisson's ratio in auxetic honeycombs. J Sandwich Struct Mater 2016. http://journals.sagepub.com/doi/pdf/10.1177/1099636216674729.

[30] Ghaznavi A, Shariyat M. Non-linear layerwise dynamic response analysis of sandwich plates with soft auxetic cores and embedded SMA wires experiencing cyclic loadings. Compos Struct 2017;171:185–97.
[31] Quan TQ, Duc ND. Nonlinear vibration and dynamic response of shear deformable imperfect functionally graded double curved shallow shells resting on elastic foundations in thermal environments. J Therm Stresses 2016;39(4):437–59.
[32] Duc ND, Quan TQ. Nonlinear dynamic analysis of imperfect FGM double curved thin shallow shells with temperature-dependent properties on elastic foundation. J Vib Control 2015;21(7):1340–62.
[33] Chorfi SM, Houmat A. Nonlinear free vibration of a functionally graded doubly curved shallow shell of elliptical planform. Compos Struct 2010;92:2573–81.
[34] Bich DH, Duc ND, Quan TQ. Nonlinear vibration of imperfect eccentrically stiffener functionally graded double curved shallow shells resting on elastic foundation using the first order shear deformation theory. Int J Mech Sci 2014;80:16–28.
[35] Quan TQ, Bich DH, Duc ND. Nonlinear analysis on flutter of functional graded cylindrical panels on elastic foundations using the Ilyushin nonlinear supersonic aerodynamic theory. J Sci: Math- Phys Vietnam Natl Univ, Hanoi 2015;31(2):1–14.
[36] Duc ND. Nonlinear dynamic response of imperfect eccentrically stiffened FGM double curved shallow shells on elastic foundation. J Compos Struct 2013;102:306–14.
[37] Duc ND. Nonlinear static and dynamic stability of functionally graded plates and shells. Hanoi: Vietnam National University Press; 2014.
[38] Reddy JN. Mechanics of laminated composite plates and shells; theory and analysis. Boca Raton: CRC Press; 2004.